Hindawi
Shock and Vibration
Volume 2022, Article ID 2224198, 9 pages
https://doi.org/10.1155/2022/2224198

Research Article

Study on Response and Influencing Factors of Shield Single/Twin Tunnel under Seismic Loading using FLAC 3D

Song Li,[1] Yanxiang Chen,[2] Linhua Huang,[1] and Enping Guo[1]

[1]*School of Civil and Environmental Engineering, Hunan University of Science and Engineering, Yongzhou, Hunan 425199, China*
[2]*College of Civil Engineering and Architecture, Guangxi University, Nanning, Guangxi 530004, China*

Correspondence should be addressed to Linhua Huang; huanglinhua@huse.edu.cn and Enping Guo; guoenping@huse.edu.cn

Received 8 February 2022; Revised 7 March 2022; Accepted 8 March 2022; Published 4 May 2022

Academic Editor: Chongqiang Zhu

The research on the dynamic response and influencing factors of shield tunnel lining under earthquake demonstrates significant engineering value in guiding the design of antiseismic tunnels. In this paper, a nonlinear finite element model of soil-tunnel interaction is established based on FLAC finite difference software, and then Mohr–Coulomb elastoplastic model and dynamic plastic damage model are used to simulate the dynamic characteristics of soil and lining damage of tunnel, and the seismic waves of South Iceland are selected to analyze the residual internal force, dynamic internal force distribution, and the relative deformation of the top and bottom of the arch of the shield tunnel under the earthquake load. Meanwhile, the effects of depth tunnel, lining thickness, and tunnel diameter on the dynamic response of the tunnel are discussed. In addition, the interaction law of horizontal parallel tunnel and the amplification effect on the surface acceleration are also studied. The results show that under the action of a strong earthquake, the bearing capacity of the tunnel decreases sharply, the lining is destroyed, and a large residual internal force appears. When the buried depth of the tunnel is small, the nonlinear effect is more significant, and the R value increases at first and then decreases with the increase in the seismic acceleration. The maximum dynamic bending moment and maximum dynamic axial force of the tunnel lining aggrandize obviously with the increase in tunnel diameter and lining thickness. In particular, the dynamic bending moment has internal force redistribution and deflection under the condition of large tunnel diameter and small lining thickness. Moreover, the interaction of parallel tunnels affects the distribution of internal force and the magnitude of adjacent surface acceleration.

1. Introduction

With the rapid development of modern transportation and the accelerated urbanization process, the problem of urban traffic congestion has become increasingly serious. An increasing number of cities have started to build underground transportation structures, such as subway tunnels and cross-river tunnels, among which shield tunnels have been widely used due to their technical and economic superiority.

According to previous research, tunnels and other underground structures have good seismic performance under conventional circumstances and can resist strong earthquake effects, so their seismic design is often neglected. However, with the construction of tunnels in high-intensity regions and changes in their diameters, embedment depths, and other parameters, underground structures such as tunnels can still produce severe damage under strong earthquake effects [1], such as the 2004 Sino-Vietnamese earthquake, when some tunnel linings collapsed in the vault [2], and the 2008 Wenchuan earthquake, when the lining of the Longxi tunnel cavern section produced ruptures in multiple directions [3]. On the other hand, due to the presence of underground structures, which change the nearby surface site conditions, seismic waves produce an amplification effect during transmission, thus affecting the seismic response of adjacent structures underground and at the surface. Numerical simulations and experimental studies have been carried out by a large number of scholars on the causes of seismic damage in tunnels and their influencing [4–6]. Wang and Cai [7] explored the dynamic response law of tunnels at different wavelength ratios by the spectral element method, and the results indicated that the velocity

amplification is proportional to the tunnel diameter, and tunnels with larger diameters are more prone to damage under seismic action. Gao et al. [8] studied the effect of burial depth on the lining stress distribution by shaking table experiments, and the experimental results demonstrated that the lining stress gradually decreases as the tunnel burial depth increases, and the lining seismic response increases significantly when the tunnel burial depth is relatively shallow, whereas the tunnel lining stress shows a gradual convergence when the burial depth reaches 40 m and above. Tao et al. [9] analyzed the dynamic characteristics of tunnels with different burial depths by shaking table tests, and their results showed that the additional bending moment generated by the tunnel structure is inversely proportional to the burial depth, so shallow buried tunnels are more prone to seismic damage compared with deeply buried tunnels. Sederat et al. [10] studied the effect of the contact interface on the elliptical deformation of circular tunnels by using quasi-static numerical analysis to obtain the lining internal forces. Kouretzis et al. [11] carried out a parametric study of shield tunnels to analyze the effect of interfacial friction on the dynamic response of the tunnel lining. Torcato [12] carried out a two-dimensional numerical simulation of the tunnel to study the effects of soil stratification around the tunnel, lining diameter, and liner thickness on the seismic response of the tunnel.

Most of the previous studies were based on shaking table tests. Although shaking table tests have the advantage of being efficient and accurate, the size of the tunnel structure model is limited by the size of the shaking table surface and the model box, and the cost of the experimental study is high. Therefore, it is of great significance to study the effect of tunnel parameters on seismic response through numerical methods. Based on the above research background, numerical models of single and parallel tunnels are developed in this paper using FLAC 3D numerical finite difference software to analyze the effects of burial depth, lining thickness, and lining diameter of a single tunnel on the seismic response of the tunnel, whilst the interaction and ground acceleration amplification effects of parallel tunnels are investigated, thus providing a theoretical reference for the application and promotion of shield tunneling technology.

2. Numerical Analysis

2.1. Numerical Model and Validation. In this paper, the numerical model is established by using FLAC 3D general finite element [13]. In order to simulate the infinite foundation conditions, the model is selected to eliminate the influence of the boundary with a larger calculation area, the model calculation domain is 180 m long and 70 m high, Figure 1 shows the grid division of the tunnel model calculation domain, the grid is gradually encrypted from the outside to the inside of the tunnel, and the grid size is based on the principle that the seismic force-frequency can be transmitted within 10 Hz [14].

To reduce the influence of seismic wave reflection at the soil subinterface and to simplify the study, the same parameters are used for all soil bodies in this paper. The dynamic response of the lining is simulated using elastic beam units, and complete bonding is assumed between the soil and the tunnel without relative slip and separation. The cumulative damage to the lining under the action of seismic forces is considered through a dynamic plastic damage model, and the calculated mechanical parameters of the tunnel and soil are shown in Table 1.

The seismic analysis of the tunnel is divided into two steps; first, the model is analyzed statically, accounting for the gravitational effect of the structure, and subsequently the dynamic analysis is performed by inputting the seismic force-time interval through the bottom of the model. The seismic loads were loaded using the 2000 South Iceland seismic acceleration timescale, and the seismic acceleration versus time curve and its power spectrum are shown in Figure 2.

Figure 3 shows the distribution of bending moment and axial force at each position of the liner under the action of seismic force. From the figure, it can be seen that the bending moment and axial force are unevenly distributed, and there are extreme value points for both bending moment and axial force at the diagonal position of positive and negative 45° of the liner, and the dynamic bending moment has the maximum value at 45°, and the dynamic axial force has the maximum value near 315°. The values of the dynamic bending moment are relatively large, while the values of dynamic axial force are relatively small. During the calculation, the soil near the tunnel is deformed, which leads to the weakening of the lining circumferential restraint effect, so when the soil deformation increases further, the dynamic bending moment also increases gradually.

Figure 4 shows the time course of bending moment and axial force of the liner at 45° position under the seismic force. From the figure, it can be seen that the time course of liner bending moment and axial force have a similar distribution pattern with the time course of seismic acceleration, and the curve of liner bending moment and axial force also fluctuates greatly near 10 s due to the sudden change of seismic acceleration. The permanent residual load of the liner was generated after the end of the applied seismic load, mainly due to the partial damage of the liner under the seismic force, which caused the reduction of the bearing capacity and made the residual internal force significant, and the residual bending moment was about 60% of the maximum moment, and the residual axial force load was about 30% of the maximum value. The residual internal force of the lining still maintains a large value after the seismic load, so the effect of residual internal force cannot be neglected when calculating the seismic response of this type.

2.2. Effect of Burial Depth on Seismic Response. According to available data, the geometric parameters of the tunnel have an important influence on the seismic dynamic response of the tunnel structure. Previous studies are usually carried out using shaking table tests, but some of the parameters cannot be accurately simulated due to the size effect, so it is important to use numerical methods to study the influence of tunnel parameters on the seismic response. Based on the

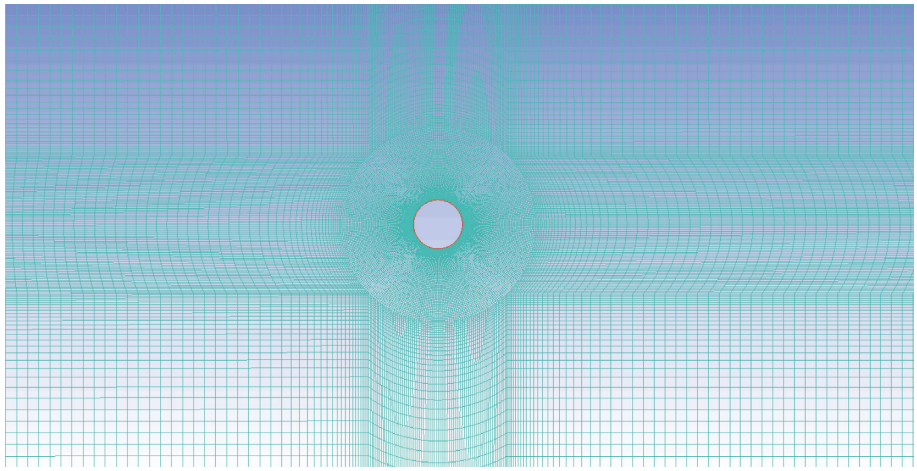

Figure 1: Model mesh of tunnel-soil.

Table 1: Parameters of tunnel and soil.

Tunnel parameters		Soil parameters	
Burial depth (m)	50	Density (kg/m^3)	2000
Diameter (m)	10	Shear wave speed (m/s)	300
Thickness (m)	0.5	Friction angle (°)	23
Density (kg/m^3)	2500	Bonding force (MPa)	0.03
Modulus of elasticity (MPa)	24.8	Poisson's ratio	0.3
Poisson's ratio	0.2	Damping ratio (%)	5

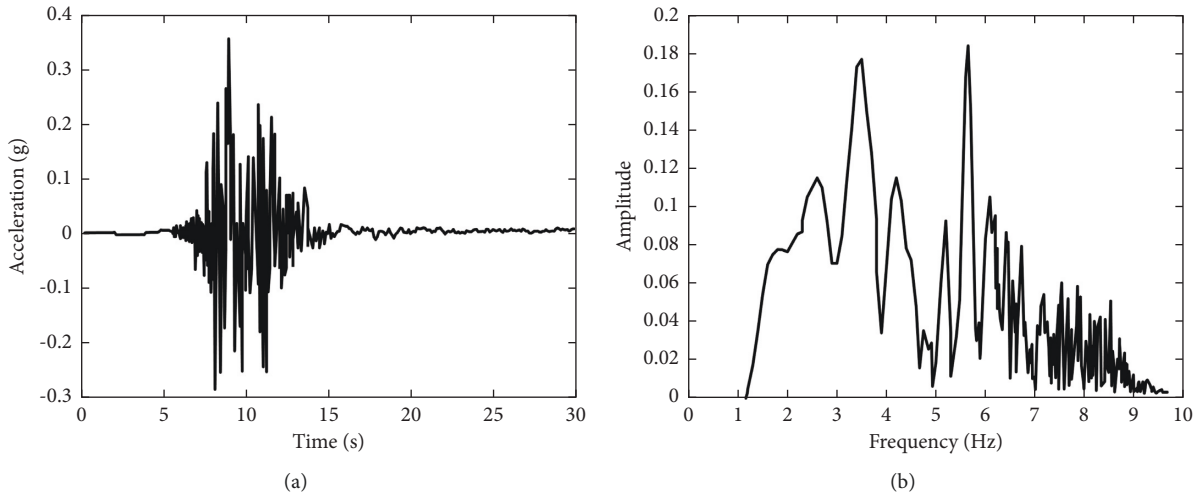

Figure 2: (a) Acceleration time history of South Iceland earthquake. (b) Power spectrum of South Iceland earthquake.

aforementioned model, this paper analyzes the effects of three parameters on the seismic response of shield tunnels by establishing tunnel models with different lining burial depths, lining thicknesses, and lining diameters.

Figure 5 shows the changes of dynamic bending moment and dynamic axial force response of the liner with different tunnel burial depths. It can be seen from the figure that the dynamic bending moment and dynamic axial force both increase with the increase in burial depth, and the distribution law of dynamic axial force is basically the same for each condition, while the distribution law of dynamic bending moment is relatively complicated. When the burial depth is shallow, the maximum dynamic bending moment of the lining appears at the right arch shoulder and left arch corner position, and with the increase in the burial depth, the dynamic bending moment fluctuates significantly along the axial direction, which may be caused by the reflection of seismic waves in the bottom area of the tunnel. The dynamic axial force shows a strong distribution pattern, and the maximum dynamic axial force at different burial depths appears near the diagonal of plus or minus 45°.

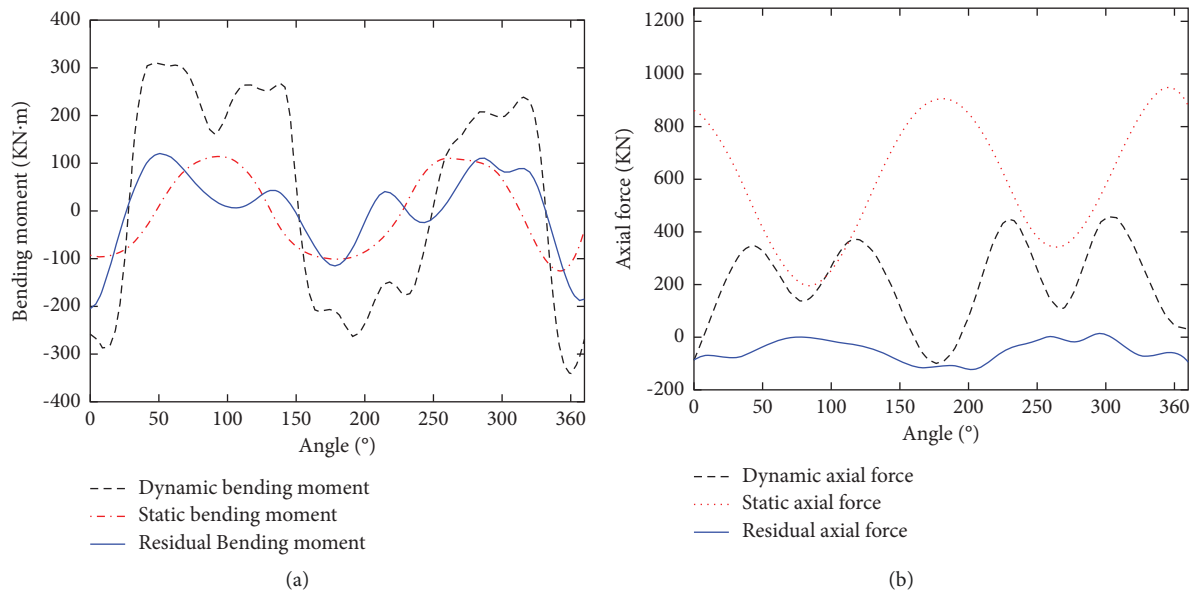

Figure 3: (a) Distribution of bending moment at each position of lining under seismic force. (b) Distribution of axial force at each position of lining under seismic force.

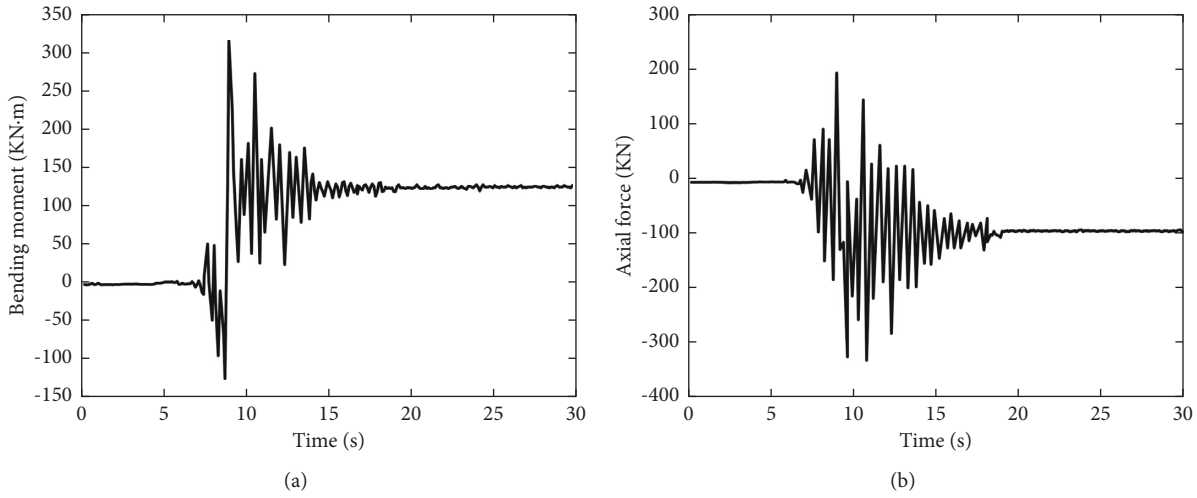

Figure 4: (a) Time history of bending moment of 45° position under seismic force. (b) Time history of axial force of lining of 45° position under seismic force.

Figure 6 shows the changes of relative displacement and R value of liner arch bottom with seismic intensity and tunnel burial depth; R value represents the ratio of relative displacement of the arch bottom to free field displacement at the same position. At the same time, the displacement of the arch top base under different burial depths is different, and the relative displacement of the arch top base is the largest when the burial depth is 35 m. With the change of seismic load acceleration, when the buried depth is large, the R value increases with the increase of seismic load intensity. When the burial depth is small, the R value increases first with the seismic acceleration and then decreases, and the maximum value of R value exists near the acceleration of 0.2 g. When the seismic load acceleration continues to increase, the R value decreases significantly. The main reason for this is that the Mohr–Coulomb principal model is used for the soil properties, and there is an amplification of the acceleration in the soil layer [15]. In addition, when the acceleration is less than 0.2 g and the burial depth is large, the calculated R value is basically around 1.0, indicating that when the tunnel is buried at a large depth, the nonlinear effect of the soil is small, and it is reasonable to use the free field method for seismic calculations.

2.3. Effect of Liner Thickness on Seismic Response. Figure 7 shows the maximum dynamic bending moment and dynamic axial force at each position under different lining thicknesses, the calculated burial depth is 12 m, and the peak ground vibration acceleration is 0.2 g. It is seen from the figure that the

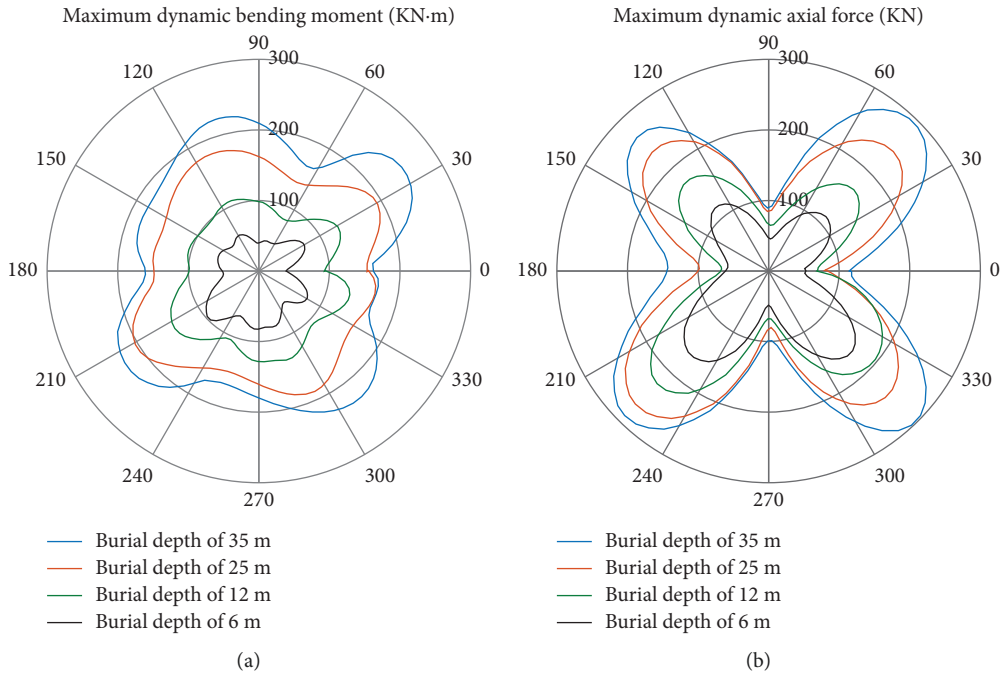

Figure 5: (a) Maximum dynamic bending moment of lining at different positions under different embedded depths. (b) Maximum dynamic axial force of lining at different positions under different embedded depths.

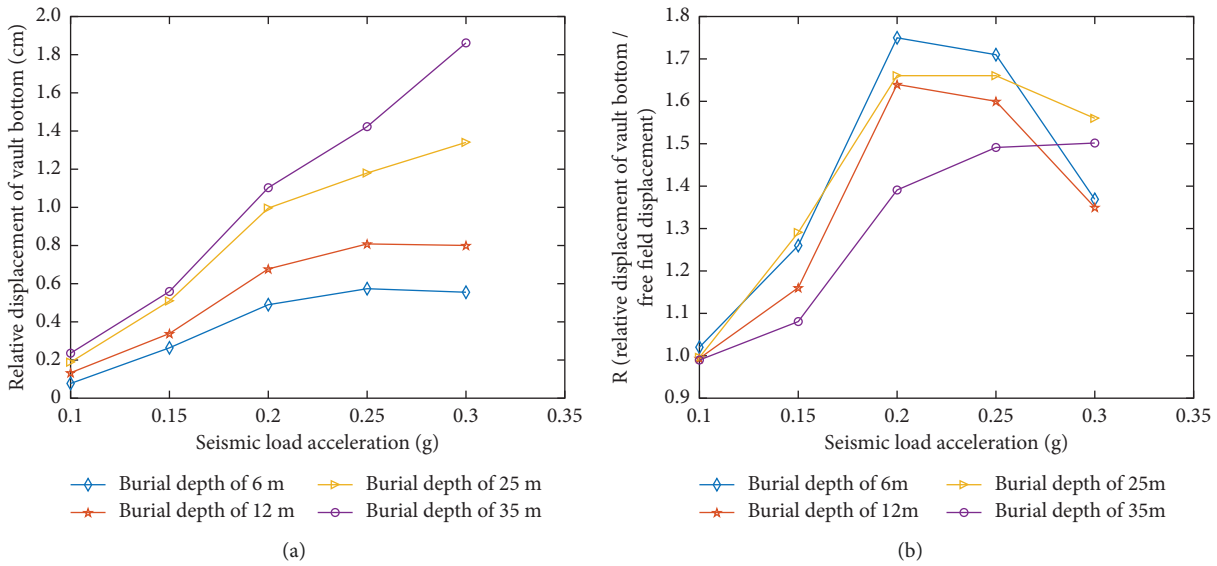

Figure 6: (a) Relative displacement of vault and bottom under different embedded tunnel depths. (b) Distribution of R value under different embedded tunnel depths.

larger the lining thickness is, the values of dynamic bending moment and dynamic axial force of the lining also increase. The distribution law of dynamic bending moment changed with the thickness, and an obvious deflection phenomenon occurred, while the distribution law of dynamic axial force did not change significantly with the thickness change. When the lining thickness is small, there are maximum dynamic bending moments at four positions of the lining 0°, 90°, 180°, and 270°, which mainly cause the redistribution of the internal forces in the lining and change the force characteristics of the tunnel [16, 17]. The distribution pattern of dynamic axial force is less affected by the lining thickness, and the maximum dynamic axial force for each condition occurs near 225° and 315° of the tunnel, and the dynamic axial force amplitude does not change significantly with the increase in lining thickness.

2.4. Effect of Liner Diameter on Seismic Response. Figure 8 shows the effect of different tunnel diameters on the dynamic bending moment and dynamic axial force under

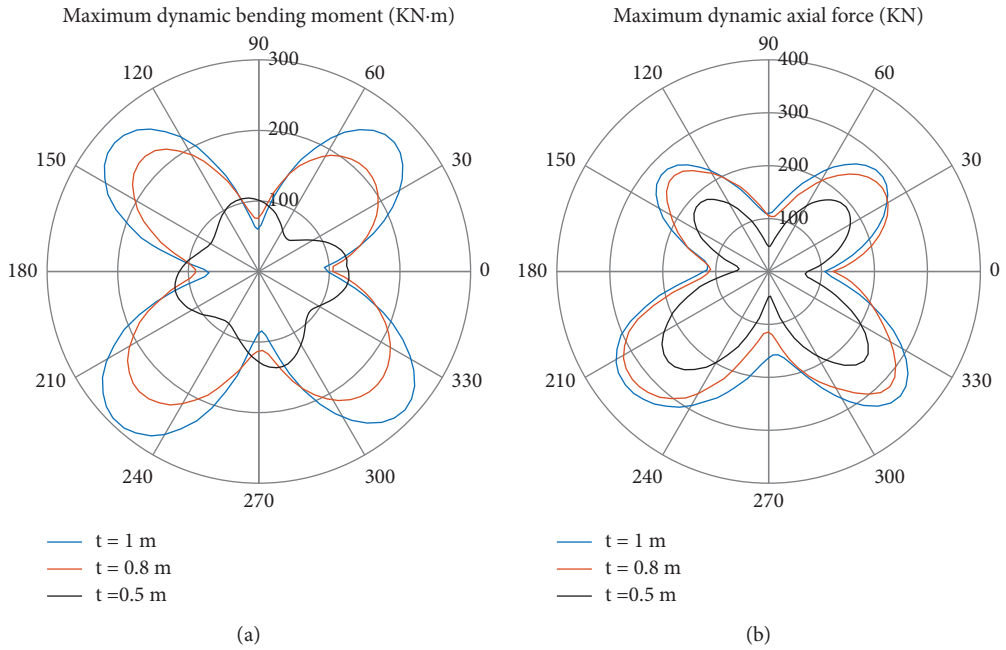

Figure 7: (a) Maximum dynamic bending moment at different positions under different lining thicknesses. (b) Maximum dynamic axial force at different positions under different lining thicknesses.

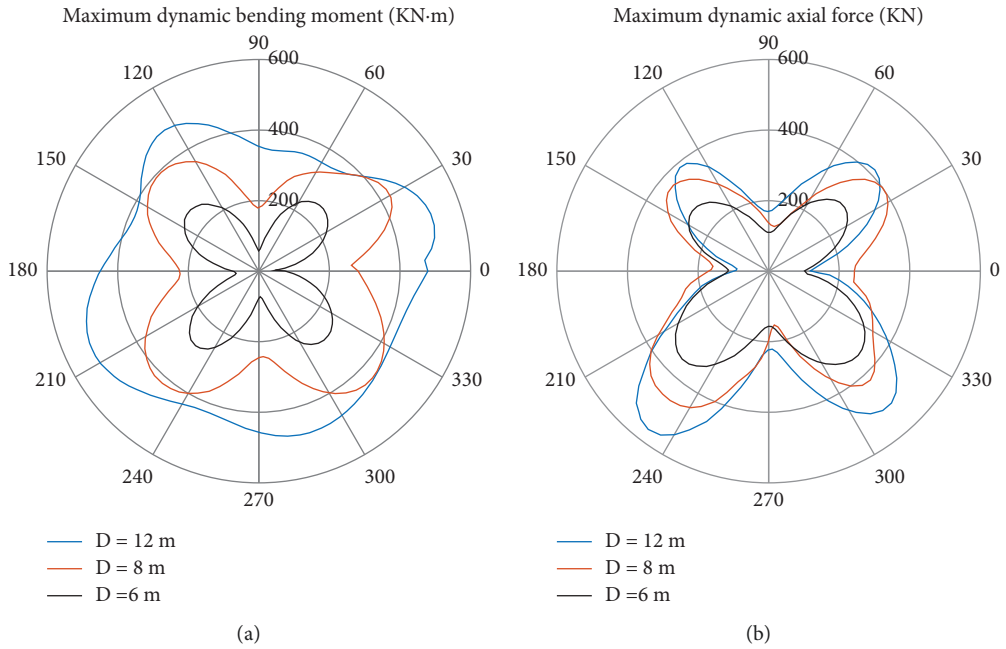

Figure 8: (a) Maximum dynamic bending moment at different positions under different lining diameters. (b) Maximum dynamic axial force at different positions under different lining diameters.

seismic forces. It can be seen from the figure that the maximum dynamic moment and the maximum dynamic axial force of the tunnel structure both increase with the diameter of the tunnel under the same seismic load, and the dynamic axial force of the lining is less affected by the diameter than the dynamic moment. When the tunnel diameter is small, the maximum dynamic bending moment is distributed at plus or minus 45°, and when the tunnel diameter is large, the dynamic bending moment distribution law becomes complex and irregular, so for large diameter shallow buried tunnel, the mechanical model simply assumes that the tunnel structure is subject to the action of far-field shear deformation and is not reasonable. The maximum dynamic axial force of the liner increases gradually with the diameter, and the change of tunnel diameter has a greater effect on the dynamic axial force at the liner arch angle

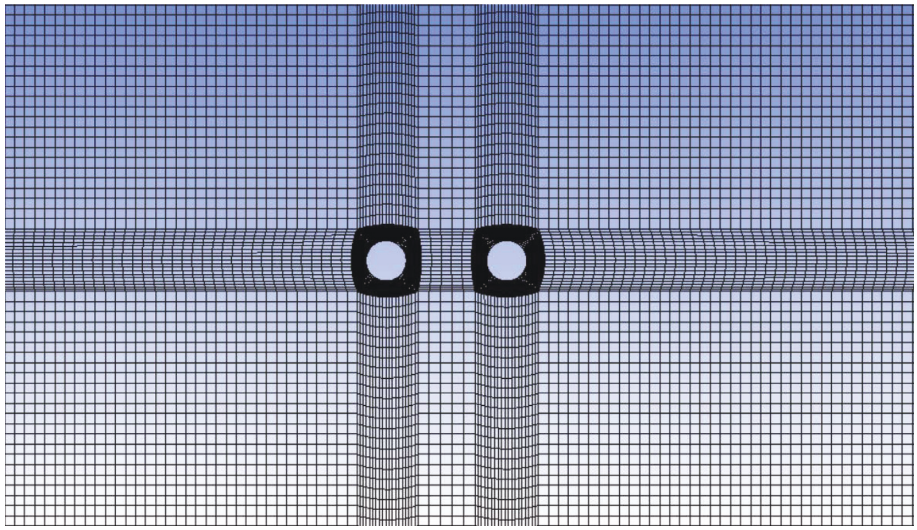

Figure 9: Model of parallel twin-tunnel and soil.

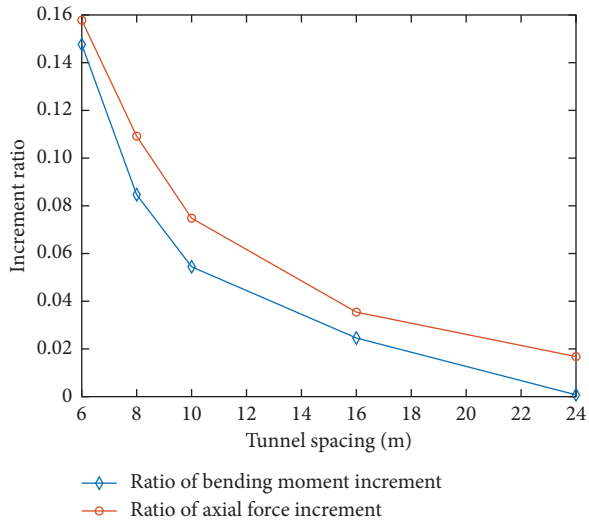

Figure 10: Ratio of internal force increment varies with spacing.

position, while the dynamic axial force at other positions is less affected by the change of diameter.

2.5. Interaction and Amplification of Parallel Tunnels under Seismic Effects. Most of the currently built shield tunnels are parallel double-row tunnels, which are more complex due to the reflection of seismic waves, and the loads on the tunnels may be significantly different compared with the single tunnel case, so it is necessary to carry out a study on the interaction effects of parallel tunnels under seismic effects [18, 19]. Based on the aforementioned study, a parallel twin-tunnel model is developed in this paper, as shown in Figure 9. The peak seismic acceleration is 0.2 g, the tunnel radius is 8 m, the lining thickness is 0.5 m, and the burial depth is 12 m, and the seismic response is calculated for five different tunnel center distances of 6 m, 8 m, 10 m, 16 m, and 24 m, respectively.

Figure 10 shows the variation of the incremental force in parallel tunnels compared with the tunnel spacing, where the incremental ratio is defined as (maximum internal force in a parallel tunnel – maximum internal force in a single tunnel)/maximum internal force in a single tunnel. As can be seen from Figure 10, with the increase in tunnel spacing, the incremental ratio of tunnel internal force gradually decreases, and the bending moment is affected more obviously compared with the axial force. When the spacing of parallel tunnels is 6 m, the incremental ratio of bending moment is about 16% and the incremental ratio of axial force is about 15%. When the spacing of tunnels is greater than 1.25 times of tunnel diameter, parallel tunnels have less influence on each other and the incremental ratio of tunnel bending moment and axial force gradually converge, and their values are less than 5%.

Under seismic loading, the presence of underground tunnels amplifies the surface shaking, and the incident waves

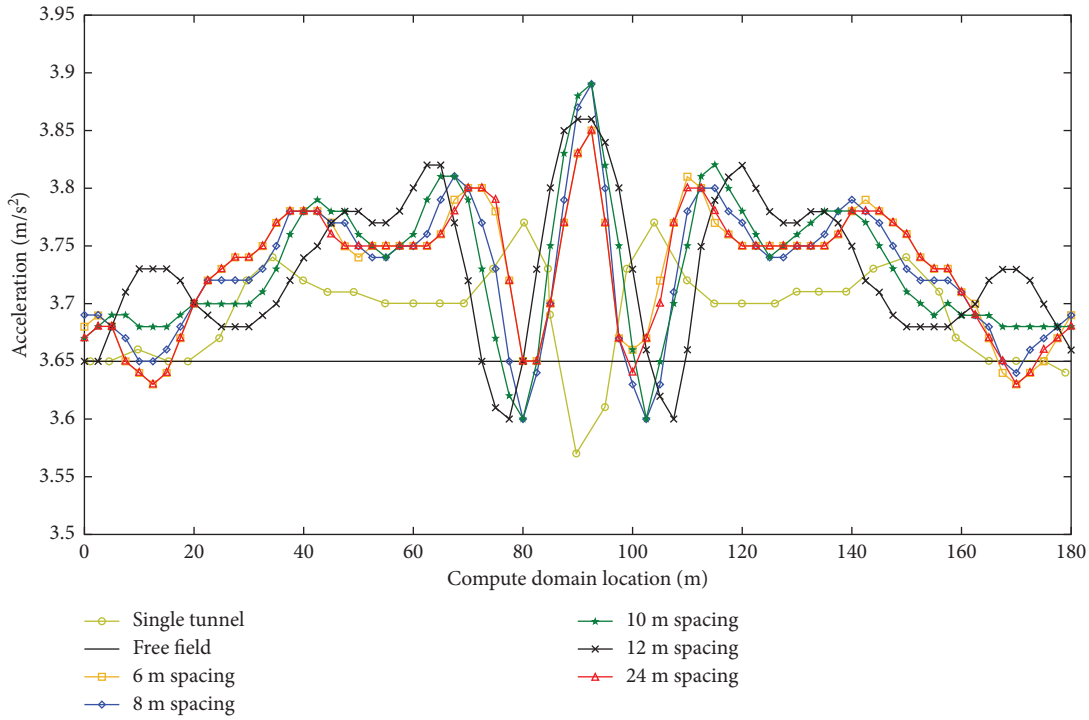

Figure 11: Comparison of peak ground acceleration.

interacting between parallel tunnels amplify this effect [20]. The amplification effect of parallel tunnels with different spacing was compared by monitoring the acceleration at the surface at the top of the computational domain. As seen in Figure 11, (1) in the single tunnel condition, the acceleration at the center of the tunnel is smaller than the free field acceleration, which is mainly due to the reflection effect at the tunnel location during the upward transmission of seismic waves, reducing the ground acceleration, while the acceleration at both sides of the tunnel increases significantly, and its maximum value increases by 3.4% compared with the free field acceleration; (2) for parallel tunnels, the acceleration directly above the tunnel is basically the same as the free field acceleration under seismic loading, and the seismic acceleration has a maximum value in the middle of the two parallel tunnels, which is 6.35% higher than the free field acceleration. The maximum accelerations calculated for parallel tunnels with different spacing are greater than the single tunnel condition, so the interaction of parallel tunnels cannot be neglected.

3. Conclusions

In this paper, a nonlinear finite element model of soil-tunnel interaction is established with a shield tunnel as the research object, and the South Iceland seismic wave curve is used to study the geometric parameters on the dynamic response of the tunnel and the interaction of parallel tunnels under the action of seismic loads, and the following conclusions are obtained through the analysis:

(1) The time course curves of bending moment and axial force of the lining under the action of seismic force coincide with the distribution pattern of South Iceland seismic acceleration time course curve, and the maximum values of bending moment and axial force appear near 10 s. The lining is damaged by the seismic force, and the bearing capacity is reduced. After the seismic load is loaded, the lining has a large residual internal force, and the residual bending moment is about 60% of the maximum bending moment and the residual axial force is about 30% of the maximum axial force.

(2) For different tunnel embedment depths, the maximum value of dynamic bending moment is at the right arch shoulder and left arch angle of the tunnel, and the maximum value of dynamic axial force appears near the plus or minus 45° diagonal. When the burial depth is larger, the R value increases with the increase in seismic load intensity. When the burial depth is smaller, the nonlinear effect is more significant, and the R value shows a trend of increasing and then decreasing with the increase in seismic load acceleration.

(3) Under the same seismic load, the maximum dynamic bending moment and maximum dynamic axial force of tunnel lining increase with the increase in tunnel diameter and lining thickness, the influence of tunnel diameter and lining thickness on dynamic axial force is smaller than that of the dynamic bending moment, the distribution of dynamic axial force under each condition is similar, and the maximum value appears around 225° and 315°. Moreover, due to inertia and plastic deformation of soil, the dynamic moments

are redistributed and deflected at larger tunnel diameters and smaller lining thicknesses.

(4) The interaction of the parallel tunnels affects their internal force distribution, which increases significantly when the spacing between the parallel tunnels is small compared with the single tunnel case. On the other hand, the presence of tunnels causes the incident waves and the reflected waves between the tunnels to superimpose on each other thus amplifying the ground acceleration, and the peak increment of ground acceleration in the middle of the parallel tunnel is doubled compared with the single tunnel case.

Data Availability

The data supporting the results of this study are obtained upon request to the corresponding author.

Conflicts of Interest

The authors declare that they have no conflicts of interest regarding the publication of this paper.

References

[1] X. Fan, G. Scaringi, O. Korup et al., "Earthquake-Induced cghpmi," *Reviews of Geophysics*, vol. 57, no. 2, pp. 421–503, 2019.

[2] H. Yu, J. Chen, A. Bobet, and Y. Yuan, "Damage observation and assessment of the Longxi tunnel during the Wenchuan earthquake," *Tunnelling and Underground Space Technology*, vol. 54, pp. 102–116, 2016.

[3] T. Li, "Failure characteristics and influence factor analysis of mountain tunnels at epicenter zones of great wenchuan earthquake," *Journal of Engineering Geology*, vol. 16, no. 6, pp. 742–750, 2008.

[4] B. Aicha, S. Mezhoud, B. Tayeb, K. Toufik, and N. Abdelkader, "Parametric study of shallow tunnel under seismic conditions for constantine motorway tunnel, Algeria," *Geotechnical & Geological Engineering*, vol. 2022, pp. 1–12, 2022.

[5] J. Wang, Y. Hu, B. Fu, H. Shan, H. Wei, and G. Cui, "Study on antiseismic effect of different thicknesses of shock absorption layer on urban shallow buried double arch rectangular tunnel," *Shock and Vibration*, vol. 2022, Article ID 4863756, 9 pages, 2022.

[6] W. Sun, Q. Ma, C. Yang et al., "Mesenchymal scealimprcem," *Immunological Investigations*, vol. 2022, pp. 1–19, 2022.

[7] X. Wang and M. Cai, "Influence of wavelength-to-excavation span ratio on ground around deep underground excavations," *Tunnelling and Underground Space Technology*, vol. 49, pp. 438–453, 2015.

[8] F. Gao, C. Sun, X. Tan, Z. Yi, and L. Hu, "Seismic response shaking table test of different buried tunnels," *Rock and Soil Mechanics*, vol. 36, no. 9, pp. 2517–2523, 2015.

[9] L. Tao, X. Qi, S. Li, H. Sen, and A. Linxuan, "Seismic dynamic response of mountain tunnel with different depth is studied by shaking table test," *Engineering seismic and reinforcement transformation*, vol. 37, no. 6, pp. 1–7, 2015.

[10] H. Sedarat, A. Kozak, Y. M. A. Hashash, A. Shamsabadi, and A. Krimotat, "Contact interface in seismic analysis of circular tunnels," *Tunnelling and Underground Space Technology*, vol. 24, no. 4, pp. 482–490, 2009.

[11] G. P. Kouretzis, S. W. Sloan, and J. P. Carter, "Effect of interface friction on tunnel liner internal forces due to seismic S- and P-wave propagation," *Soil Dynamics and Earthquake Engineering*, vol. 46, pp. 41–51, 2013.

[12] D. M. M. F. Torcato, *Seismic Behaviour of Shallow Tunnels in Stratified ground*, Univeridade Ténica de Lisboa, Lisbon, Portugal, 2010.

[13] M. Bonini, M. Barla, and G. Barla, "FLAC applications to the analysis of swelling behavior in tunnels," *FLAC and Numerical Modeling in Geomechanics*, pp. 329–333, CRC Press, Boca Raton, FL, USA, 2020.

[14] H. Li, J. Wu, J. Liu, and L. Yubing, "Finite element mesh generation and decision criteria of mesh quality," *China Mechanical Engineering*, vol. 23, no. 3, pp. 368–377, 2012.

[15] D. Fu and Y. Gu, "Research onseismic response of mountain tunnel considering soil-structure dynamic interaction," *Journal of Guangxi University(Natural Science Edition)*, vol. 44, no. 1, pp. 176–182, 2019.

[16] R. C. Gomes, "Effect of stress disturbance induced by construction on the seismic response of shallow bored tunnels," *Computers and Geotechnics*, vol. 49, pp. 338–351, 2013.

[17] Z. Zhang, B. Chen, H. Li, and H. Zhang, "The performance of mechanical characteristics and failure mode for tunnel concrete lining structure in water-rich layer," *Tunnelling and Underground Space Technology*, vol. 121, Article ID 104335, 2022.

[18] X. Jiang, W. Liu, H. Yang, J. Zhang, and L. Yu, "Study on dynamic response characteristics of slope with double-arch tunnel under seismic action," *Geotechnical & Geological Engineering*, vol. 39, no. 2, pp. 1349–1363, 2021.

[19] L. Pai and H. Wu, "Multi-attribute seismic data spectrum analysis of tunnel orthogonal underpass landslide shaking table test," *Soil Dynamics and Earthquake Engineering*, vol. 150, Article ID 106889, 2021.

[20] China Planning Press, *Gb 50909-2014, Code for Seismic Design of Urban Rail Transit Structures: GB 50909-2014*, China Planning Press, Beijing, China, 2014.